PROCEEDINGS OF SCIENCE

Weak Interaction in Nuclear Astrophysics - main actor: Gamow-Teller transitions -

Yoshitaka FUJITA*
Research Center for Nuclear Physics (RCNP)
Mihogaoka, Ibaraki, Osaka 567-0047, Japan
and
Department of Physics, Osaka University,
Machikaneyama 1-1, Toyonaka, Osaka 560-0043, Japan
E-mail: fujita@rcnp.osaka-u.ac.jp

Study of nuclear weak processes, especially the Gamow-Teller (GT) transitions, starting from stable as well as unstable nuclei, is one of the key issues in nuclear physics and nuclear astrophysics. In the collapsing core of pre-supernova stars, where the temperature of a few $\times 10^9$ K is expected, electron capture and neutrino induced reactions play important roles. In these reactions, GT transition is one of the main actors. However, due to the weakness of the weak interaction causing these reactions, experimental study of these reactions that can happen under such extreme stellar conditions are difficult. Direct information on GT transitions and the GT transition strength B(GT) by using the weak interaction itself has been available only from β-decay measurements. However, B(GT) values are usually derived only for low-lying states. Note that the study of the feedings to higher excited states is difficult in a β-decay study, because the phase-space factor (f-factor) decreases with the excitation energy.

The GT transitions are caused by the $\sigma\tau$-type operator. It is known that the nuclear excitation by means of the $\sigma\tau$-type nuclear strong interaction becomes dominant in charge-exchange (CE) reactions performed at small scattering angles and intermediate incident energies. Therefore, we study the GT transitions using hadronic (^{3}He,t), CE reactions. By realizing dispersion matching conditions, high energy-resolution has been realized and detailed GT strength distributions can be studied up to high excitation energies.

Under the assumption that isospin is a good quantum number, symmetry is expected for the structure of mirror nuclei and the GT transitions starting from them. The results from (^{3}He,t) reactions on stable pf-shell nuclei are compared and also combined with the complementary β-decay studies for the mirror proton-rich nuclei in the region far-from-stability. Since the pass of the rp-process nucleosynthesis goes thorough these proton-rich nuclei, the information on GT transitions from them are essential for the better understanding of the process.

VI European Summer School on Experimental Nuclear Astrophysics, ENAS 6
September 18-27, 2011
Acireale, Italy

*Speaker.

PoS(ENAS 6)031

1. Introduction

Gamow-Teller (GT) transition is the most common weak interaction process of spin-isospin ($\sigma\tau$) type in atomic nuclei [1]. They are of interest not only in nuclear physics, but also in astrophysics [2, 3]; they play important roles, for example, in the core-collapse stage of type II supernovae and nucleosynthesis. The direct study of weak decay processes, however, gives relatively limited information about GT transitions and the states excited via GT transitions (GT states); β decay can only access states at excitation energies lower than the decay Q-value, and neutrino-induced reactions have very small cross-sections. However, one should note that β decay has a direct access to the absolute GT transition strength B(GT) from a study of half-lives, Q_β-values, and branching ratios.

In contrast, the complementary charge-exchange (CE) reactions, such as (p,n) or $(^3\mathrm{He},t)$ reactions at intermediate beam energies and 0°, can selectively excite GT states up to high excitation energies in the final nucleus. In recent $(^3\mathrm{He},t)$ measurements, one order-of-magnitude improvement in the energy resolution has been achieved. This has made it possible to make one-to-one comparison of GT transitions studied in $(^3\mathrm{He},t)$ reactions and β decays. In addition, it was found that there is a good proportionality between the cross-sections at 0° and the B(GT) values. Thus, cross-sections of GT states observed in $(^3\mathrm{He},t)$ reactions can be normalized by the β-decay results to obtain B(GT) values up to high excitation energies.

In this report, we study first the basic properties of GT transitions and then the properties of "operators" that distinguish the different modes of nuclear excitations. As a result, we see the "unique position" of the GT excitation among various excitation modes. By understanding the meaning and the importance of the reduced transition strength B(GT), we will see how the studies by β decay caused by the weak interaction and CE reactions caused by the strong interaction are connected through the B(GT) value. We will also see that the effort to combine the results from these two methods under the assumption of "isospin symmetry" in nuclei is important. A brief overview of GT transition strengths, the so-called "GT response functions", is presented for some light to heavy nuclei.

2. Properties of Gamow-Teller Transitions

The name "Gamow-Teller" of the GT transition naturally comes from the name of the "allowed" transitions observed in β decays. The GT transitions have spin-flip ($\Delta S = 1$) nature and are caused by the $\sigma\tau$-type operator. The main features of GT transitions can be summarized as follows:

(1) They start from a nucleus with Z and N and lead to states in a neighboring nucleus with $Z \pm 1$ and $N \mp 1$. Thus the β^+-type GT transitions have the nature of $\Delta T_z = +1$ and the β^--type GT transitions $\Delta T_z = -1$, where T_z is defined by $(N-Z)/2$ and is the z component of the isospin T. As a result, they are of isovector (IV) nature with ΔT = **1** ($\Delta T = \pm 1$ or 0). Since GT transitions involve ΔS = **1** ($\Delta S = \pm 1$ or 0) and ΔL = 0, they also have ΔJ = **1** ($\Delta J = \pm 1$ or 0) and no parity change.

(2) They can be studied either in β decay (weak interaction) or in Charge Exchange (strong interaction) reactions.

(3) Since the $\sigma\tau$ operator has no spatial component, transitions between states with similar spatial shapes are favored.
(4) In a simple, independent-particle picture where the individual nucleons are in an orbit with orbital angular momentum ℓ and spin s, a GT transition connects initial and final states with the same ℓ. Therefore, the transitions are among the spin-orbit partners, i.e., the $j_>$ ($=\ell+1/2$) and the $j_<$ ($=\ell-1/2$) orbits. The $j_> \leftrightarrow j_<$ transition and the transitions between the same orbits (i.e., $j_> \leftrightarrow j_>$ and $j_< \leftrightarrow j_<$) are separated, in first order, by 3 to 6 MeV, the separation in energy of the spin-orbit partners.
(5) In contrast to the Fermi transitions, where only the T_z is changed by the τ operator and hence only a single state [the so-called Isobaric Analog State (IAS)] is populated in the final nucleus, GT transitions involve both the σ and the τ operators and a variety of different states can be populated. As a result one can extract more information about nuclear structure in the final nucleus.
(6) Besides the information on nuclear structure, GT transitions are also important in terms of our understanding of many processes in nuclear astrophysics.

On the assumption that the nuclear interaction is charge-symmetric, isospin is a good quantum number. As a result, isobars with $\pm T_z$ should exhibit a symmetric structure. Therefore, corresponding (analogous) GT transitions with, for example, $T_z = \pm 1 \rightarrow 0$ and $T_z = \pm 2 \rightarrow \pm 1$ are expected to have the same transition strengths. They can be studied by charge-exchange (CE) reactions and β decay [4]. It should be noted that the relative GT strengths can be well studied up to high excitation energies in CE reactions, but the absolute B(GT) strengths are obtained by normalizing to those obtained in β-decay studies. Thus, studies of β-decay and CE reactions are complementary.

3. Nuclear Excitations

In order to understand how the strengths of GT transitions can be studied by using β decay and CE reactions, we start from the fundamental idea on the properties of simple "one-particle - one-hole ($1p$-$1h$)"-type nuclear excitations and the "operators" associated with individual excitation modes. We also study the importance of the reduced transition strengths denoted by $B(Op)$, where Op stands for the names of operators.

Nuclei is unique in the sense that three interactions out of four fundamental interactions are active, i.e., strong, electro-magnetic (EM), and weak interactions. Nuclei can be defined as the "quantum finite many-body system", in which nucleon degrees of freedom (i.e., proton and neutron degrees of freedom) are treated apparently, while meson, photon, and boson degrees of freedom are treated indirectly as the means to transmit strong, EM, and weak interactions, respectively. By means of these interactions that are active in nuclei, various modes of nuclear excitations can be caused and each of them can be of interest in nuclear astrophysics.

If a proper amount of energy is given to a nucleus, the simplest excitation that can happen is $1p$-$1h$ type assuming that nuclei have shell structure. The given energy is used to excite a proton or a neutron from the initial shell, leaving "one hole" in it, to a higher energy empty shell, creating "one particle". The energy can be given to the nucleus by nuclear reactions caused by hadrons or leptons or absorption of photons. Even a β decay gives energy accumulated in the initial (mother) nucleus to the final (daughter) nucleus and causes $1p$-$1h$ excitations of "one proton-particle and one neutron-hole" or "one neutron-particle and one proton-hole" in the final nucleus. It should be noted

that 1p-1h excitations with the same structure (under the assumption of isospin symmetry) can be created by CE reactions, although β decay is caused by the weak interaction, while CE reaction by the strong interaction. We know that Fermi and GT transitions are dominant in β decays. They are caused by the operators of τ and $\sigma\tau$ type, respectively. The excitations caused by these operators are called Fermi and GT modes, respectively. Therefore, each excitation mode is characterized by an operator that excites the specific mode. Here, we first discuss the "mode" of 1p-1h type nuclear excitations.

3.1 Mode of Excitation

A 1p-1h type excitation is interpreted as a high-frequency surface vibration of a nucleus, if we think of a phenomenological liquid drop model of a nucleus. There, a naive picture of the vibration is the one-phonon excitation on the surface of a viscous liquid drop consisting of nuclear matter. When 1p-1h excitations with various configurations participate "in phase" in the vibration, such one-phonon excitation has the "collective" nature. Collective excitations observed at excitation energies around or higher than 10 MeV are called giant resonances (GRs). The degree of collectivity is denoted by how much of the fraction of the total vibrational amplitude allowed for each mode, called "sum rule" limit value, is observed in a state having usually a broad bump-like structure. It should be noted that the excitation energy E_x of 10 MeV corresponds to an oscillation frequency of $\approx 10^{21}$ Hz, which is one of the fastest vibrations of many-body quantum systems.

Since a nucleus is a "quantum system", each excitation mode, similar to other excitation modes of a quantum system, is distinguished by a few quantum numbers. Representative quantum numbers are angular momentum L, spin S, and isospin T as summarized in Fig. 1.

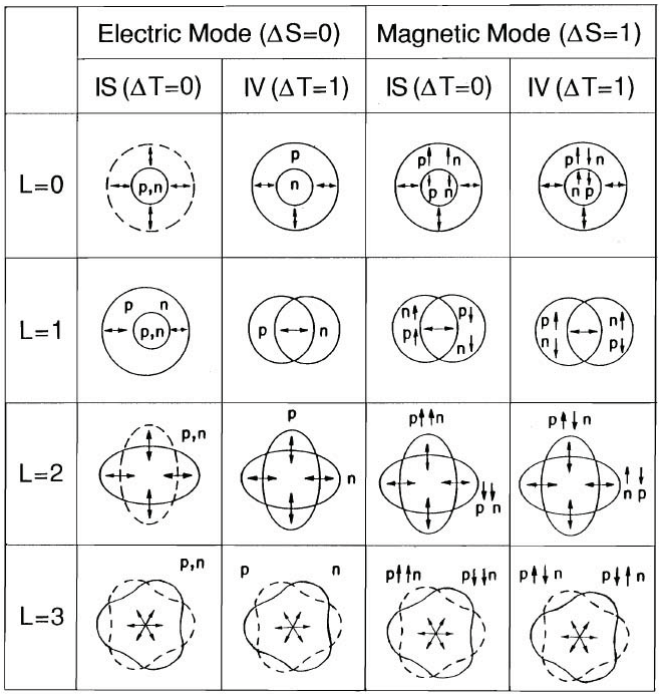

Figure 1: Illustration of various excitation modes in nuclei. Each mode is identified by the angular momentum (transfer) L, association (or not) of spin excitation ΔS and association (or not) of isospin excitation ΔT. Illustrations show the excitations on the ground state (g.s) of an even-even (Z,N), spherical nucleus, for simplicity.

Under the assumption of liquid drop model, we can have the image that various nuclear excitations with different angular momenta have different shapes of vibration. The excitation modes

with an angular momentum (transfer) $L = 0$ are called "monopole modes", the $L = 1$ ones "dipole modes", the $L = 2$ ones "quadrupole modes", and so on. Note that only if the excitation is on a $J^\pi = 0^+$, even-even nucleus, "angular momentum" of the excitation and "angular momentum transfer" in a reaction (or a decay) have the same L value.

In this simple picture, those modes that are associated with isospin excitation, i.e., an excitation in which protons and neutrons oscillate out of phase, are called "isovector (IV) modes" while those without isospin excitation, i.e., protons and neutrons oscillate in phase, are called "isoscalar (IS) modes".

In the multipole decomposition of the EM transitions (γ transitions), the transitions not associated with spin excitation ($\Delta S = 0$) are called the electric transitions and those with spin excitation ($\Delta S = 1$) are called the magnetic transitions. Depending on the amount of total angular momentum transfer λ, they are called the $E\lambda$ and $M\lambda$ transitions, respectively.

By analogy with the electric modes of γ transitions, nuclear excitations (and also the corresponding GRs) that are not associated with spin excitation are called "electric modes" and those with the total angular momentum transfer λ are called "$E\lambda$ modes". An $E\lambda$ mode is further categorized into IS and IV modes (see Fig. 1). Since $\Delta S = 0$ in $E\lambda$ modes, λ is the same as the momentum transfer L. The IS, $E\lambda$ modes, such as $E0$ or $E2$ modes are excited and clearly observed in inelastic reactions caused by spin-less particles, such as α inelastic scattering [(α, α') reaction].

Nuclear excitations associated with spin excitation, i.e., with an image of spin-up nucleons and spin-down nucleons oscillate out of phase, are called "magnetic modes". However, the names "$M\lambda$ modes" are mainly used for the excitations observed in reactions using EM probes, such as (e, e') or (γ, γ'), because the operators that excite $M\lambda$ modes are common with those of γ transitions. The magnetic modes induced by hadron inelastic scatterings are usually called by more direct names. For example, the $L = 0$, and $\Delta S = 1$ excitation is called the spin-$M1$ mode and the $L = 1$, $\Delta S = 1$ excitation is called the spin-dipole mode.

Note that the names "electric mode" or "magnetic mode" are usually used only for the inelastic-type excitations (including photo absorption) due to the analogy with γ transitions connecting two states inside a nucleus.

Since GT excitation is with $L = 0$, $\Delta S = 1$, and $\Delta T = 1$, it is represented by the image shown in the right upper panel of Fig. 1. It is a doubly folded vibration; spin up and spin down particles oscillate out of phase, and proton and neutron also oscillate out of phase. We, however, notice that the spin-$M1$ mode, which is not associated with charge exchange, is also represented by the same image. We will see that they can be distinguished only by the difference of the type of operators that causes these excitations.

3.2 Operators and the Excitation Modes

For a quantum system such as nucleus, we should note that a visual image of a mode is not always correct nor clear, especially when the mode is associated with spin or isospin excitations. For example, excitations by β decays or CE reactions cannot be properly described. In these cases in which quantum numbers specific to quantum mechanics are involved, we have to come back to a basic view point that each $1p$-$1h$ excitation is caused by the action of an interaction described by

a specific operator. Thus, each mode of excitation should be distinguished by the type of operator exciting the mode.

For the simplest cases of IS electric transitions, it is usual to assume a type of operator [5, 6] with the form

$$O(Lm) = (Z/A)\sum_i r_i^L Y_m^L(\Omega), \;\; L \geq 2, \tag{3.1}$$

where the summation runs over all the nucleons i, and L is the angular momentum transfer of the transition, r is the radial operator, and Y_m^L is the spherical harmonic operator.

The IV-type operators are associated with a "τ" operator which can change isospin T. In addition, "σ" operator which can flip spin S is in magnetic-type operators. The simplest excitation modes associated with both τ and σ operators are the spin-$M1$ and GT modes with an angular momentum transfer $L = 0$. Their operators have the shape

$$O(M1) = \frac{1}{\sqrt{2}}\sum_i \sigma_i \tau_i^0 \qquad \text{and} \qquad O(\mathrm{GT}^{\pm 1}) = \frac{1}{\sqrt{2}}\sum_i \sigma_i \tau_i^{\pm 1}, \tag{3.2}$$

where τ_i^0 is the operator that does not change the z-component of the isospin T_z defined by $1/2(N-Z)$. Therefore, the spin-$M1$ excitation is inside the nucleus specified by (Z,N). On the other hand, $\tau_i^{\pm 1}$ in the GT operator are the raising and the lowering operators, respectively, that changes the T_z by ± 1 and thus causing excitations (or decay) in the β^+ and β^- directions. Therefore, the final nuclei have $(Z-1,N+1)$ and $(Z+1,N-1)$, respectively. The $\tau_i^{\pm 1}$ operator itself is responsible for the excitation of the isobaric analog state (IAS) by means of the Fermi transition.

The essential part of the operators corresponding to the oscillations shown in each panel of Fig. 1 is given in Fig. 2. It is always important to think of an operator (or an active interaction) causing the specific excitation in mind, in addition to having a visual image of oscillation shape given in Fig. 1.

In the simplest shell model assuming a harmonic-oscillator (HO) potential, states with the main quantum number N $(= 0, 1, 2, ..)$ have an energy of "$N\hbar\omega$", where the value of $1\hbar\omega$ depends on mass number A and is $\approx 41/A^{1/3}$. The parity associated with N is $(-)^N$. The values of orbital angular momentum ℓ allowed in the Nth state should be smaller than N and the parity associated with ℓ is $(-)^\ell$. Therefore, allowed ℓ values are restricted to $\ell = N, N-2, ...$

In making $1p$-$1h$ excitations by the $r^n Y_m^L$ type operator, we see that the operator r^n can change the main quantum number N maximally by n units. In addition, L should be smaller than n. Since the parity change is determined by $(-)^n$, the r^n operator with the even n values are accompanied by the Y_m^L operators with even L vales. As a result, excitations with even $\hbar\omega$ values are expected for the even L excitations. The same is true for the odd L excitations. Therefore, we see that the minimum n is L and $n = L+2, L+4, ..$ are also allowed. At the same time, if we think of the condition that the parity associated with N is $(-)^N$, we see that ΔN can be n or $n-2, n-4, ..$, but larger than 0. This is illustrated in Fig. 3.

For example, $E2$ (electric quadrupole) excitation with an even L transfer of two and caused by the $r^2 Y_m^2$ type operator can have strengths at $\Delta N = 2$ ($2\hbar\omega$ jump) and also at $\Delta N = 0$ ($0\hbar\omega$ jump). On the other hand, $E3$ (electric octupole) excitation with an odd L transfer of three and caused by the $r^3 Y_m^3$ type operator have strengths at $\Delta N = 3$ ($3\hbar\omega$ jump) and also at $\Delta N = 1$ ($1\hbar\omega$ jump).

	$\Delta S=0$ $\Delta T=0$	$\Delta S=0$ $\Delta T=1$	$\Delta S=1$ $\Delta T=0$	$\Delta S=1$ $\Delta T=1$
L = 0		$\sum \tau_i$ IAS		$\sum \vec{\sigma}_i \tau_i$ GTR
2nd order	$\sum r_i^2$ ISGMR	$\sum r_i^2 \tau_i$ IVGMR	$\sum r_i^2 \vec{\sigma}_i$ ISSMR	$\sum r_i^2 \vec{\sigma}_i \tau_i$ IVSMR
L = 1		$\sum r_i Y_m^1 \tau_i$ IVGDR	$\sum r_i Y_m^1 \vec{\sigma}_i$ ISSDR	$\sum r_i Y_m^1 \vec{\sigma}_i \tau_i$ IVSDR
2nd order	$\sum r_i^3 Y_m^1$ ISGDR			
L = 2	$\sum r_i^2 Y_m^2$ ISGQR	$\sum r_i^2 Y_m^2 \tau_i$ IVGQR	$\sum r_i^2 Y_m^2 \vec{\sigma}_i$ ISSQR	$\sum r_i^2 Y_m^2 \vec{\sigma}_i \tau_i$ IVSQR
L = 3	$\sum r_i^3 Y_m^3$ ISGOR	$\sum r_i^3 Y_m^3 \tau_i$ IVGOR	$\sum r_i^3 Y_m^3 \vec{\sigma}_i$ ISSOR	$\sum r_i^3 Y_m^3 \vec{\sigma}_i \tau_i$ IVSOR

Figure 2: Operators that excite representative "vibrational" nuclear excitation modes. The giant resonances (GRs) corresponding to these vibrational modes are given by their abbreviated names. (courtesy of J. Jänecke.) They are: IAS, isobaric analog state; GTR, Gamow-Teller resonance; ISGMR, isoscalar giant monopole resonance; IVGMR, isovector giant monopole resonance; ISSMR, isoscalar spin monopole resonance; IVSMR, isovector spin monopole resonance; IVGDR, isovector giant dipole resonance; ISSDR, isoscalar spin dipole resonance; IVSDR, isovector spin dipole resonance; ISGDR, isoscalar giant dipole resonance; ISGQR, isoscalar giant quadrupole resonance; IVGQR, isovector giant quadrupole resonance; ISSQR, isoscalar spin quadrupole resonance; IVSQR, isovector spin quadrupole resonance; ISGOR, isoscalar giant octupole resonance; IVGOR, isovector giant octupole resonance; ISSOR, isoscalar spin octupole resonance; IVSOR, isovector spin octupole resonance. This list is not complete. Some of them have not yet been found experimentally (see Ref. [6]).

A detailed microscopic descriptions of excitation modes and GRs can be found in a book "Giant Resonance" [6].

It should be noted that the excitations of IAS and GT mode are not associated with the radial operator r. Therefore, they can be categorized as the modes of "$0\hbar\omega$" excitation. However, the excitation energy of the IAS can be zero, but also more than 10 MeV due to the large difference of the Coulomb energy in the mother (Z,N) nucleus and the daughter $(Z+1,N-1)$ nucleus, especially as the mass number Z becomes large. The same is true for the GT mode. The center of the gravity of the excitation strength can be sometimes found at less than $E_x = 1$ MeV in some nuclei such as ^{18}F and ^{42}Sc in the β decay study of ^{18}Ne and ^{42}Ti or the $(^3\mathrm{He},t)$ study on ^{18}O and ^{42}Ca nuclei, but in many cases at ≈ 10 MeV in heavier nuclei. As will be shown in later sections, strength distributions of GT modes are largely affected by the structure of individual nuclei, which makes the study of GT transitions interesting [4]. At the same time, predictions of GT strength distributions are difficult. Honest effort of step-by-step is needed for the study of GT transitions.

3.3 β decay and the Reduced Gamow-Teller Transition Strength B(GT)

In β-decay experiments, the reduced GT transition strength, the B(GT) value for a GT transi-

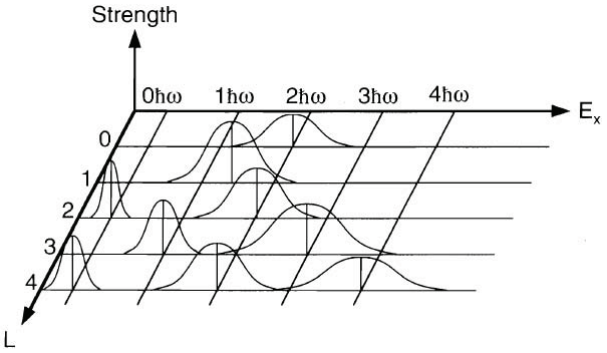

Figure 3: Schematic idea of strength distributions of nuclear excitations with angular momentum transfer of $L = 0$ to 4. The $L = 0$ strength distribution is shown for the ISGMR. Due to the r^2 nature of its operator, the main part of the strength is expected at $E_x = 2\hbar\omega$. The $L = 1$ strength distribution is shown for the IVGDR. Due to the "repulsive" nature of the IV mode, the excitation energy is higher than the expected value of $1\hbar\omega$. For the modes with even L values of 2 and 4, strengths are distributed at $0\hbar\omega$ and $2\hbar\omega$ excitations, and at $0\hbar\omega$, $2\hbar\omega$, and $4\hbar\omega$ excitations, respectively. On the other hand, for the mode with odd L value of 3, strengths are at $1\hbar\omega$ and $3\hbar\omega$ excitations. For the detail, see text. The IAS and GT modes excited by CE processes have the nature of "$0\hbar\omega$" excitation due to the lack of radial operator r. The excitation energies of them are largely dependent on the structures of initial and final nuclei.

tion to a level j with an excitation energy E_j is expressed in terms of the $f_j t_j$ value, where t_j is the partial half-life to level j and f_j is the phase-space factor. Similarly, the Fermi transition strength, B(F), is related to the partial Fermi half-life $t_{\rm F}$ and $f_{\rm F}$. Thus, we have the relationships

$$B_j(\mathrm{GT})\lambda^2 = K/f_j t_j \quad \text{and} \quad B(\mathrm{F})(1-\delta_c) = K/f_{\rm F} t_{\rm F}, \tag{3.3}$$

where $K = 6143.6(17)$ [7], $\lambda = g_A/g_V = -1.270(3)$ [8] and δ_c is the Coulomb correction factor [9].

The GT part of Eq. (3.3) can also written as

$$1/t_j = (\lambda^2/K) f_j B_j(\mathrm{GT}). \tag{3.4}$$

Since we know that the value $1/t_j$ shows how fast the transition proceeds, i.e., the transition strength, and f_j is a kind of kinematical factor calculated from the energy allowed for each GT transition (Q value for the jth β decay), this equation simply shows that the transition strength is proportional to B(GT) value.

The reduced GT transition strength B(GT) for the transition from the initial state with spin J_i, isospin T_i, and z-component of isospin T_{zi} to the final state with J_f, T_f, and T_{zf} is given by [10]

$$B^{\pm1}(\mathrm{GT}) = \frac{1}{2J_i+1}\left|\langle J_f T_f T_{zf} \| \frac{1}{\sqrt{2}} \sum_{j=1}^{A} (\sigma_j \tau_j^{\pm1}) \| J_i T_i T_{zi}\rangle\right|^2, \tag{3.5}$$

where $\tau^{\pm1} = \mp(1/\sqrt{2})(\tau_x \pm i\tau_y)$ and transforms as a tensor of rank one. By applying the Wigner-Eckart theorem [11] in isospin space, we get

$$B(\mathrm{GT}) = \frac{1}{2J_i+1}\,\frac{1}{2}\,\frac{C_{\rm GT}^2}{2T_f+1}\left|\langle J_f T_f \| \sum_{j=1}^{A} (\sigma_j \tau_j) \| J_i T_i\rangle\right|^2 \tag{3.6}$$

$$= \frac{1}{2J_i+1}\,\frac{1}{2}\,\frac{C_{\rm GT}^2}{2T_f+1}\left[M_{\rm GT}(\sigma\tau)\right]^2, \tag{3.7}$$

where $C_{\rm GT}$ is the isospin Clebsch-Gordan (CG) coefficient $(T_i T_{zi} 1 \pm 1 | T_f T_{zf})$, and the $M_{\rm GT}(\sigma\tau)$ is the IV spin-type GT matrix element [4]. From this expression for the "reduced" GT transition strength, we note that B(GT) consists of the squared value of the transition matrix element for the operator $\sigma\tau$ and the spin and isospin geometrical factors.

Here, important is to note that the transition rate of a process caused by the weak interaction (for example, β decay) can be calculated once the squared value of the transition matrix element, or more directly the B(GT) value, is obtained. This simple relationship comes from the fact that the mechanism caused by the weak interaction is very simple, because weak processes happen at a δ-function-like "point" in space, because W and Z bosons having extremely heavy masses are exchanged in them. We know that the uncertainty principle makes the life-time of the bosons very short and thus the effective range of the weak interaction. (Details of β-decay studies can be found in Ref. [12].) On the other hand, simple mechanism is not always expected in hadron-induced reactions, in which mesons, having a mass much smaller than nucleons but not negligibly small, are exchanged. Simple one-step reaction mechanism can be usually realized at incident energies of more than 100 MeV/nucleon.

4. Study of Gamow-Teller Transitions

A project to study the GT transitions in various p-shell, sd-shell, and pf-shell nuclei is in progress by combining the information obtainable from β decays and CE reactions. As discussed, the direct study of weak decay processes gives relatively limited information about GT transitions and the states excited via GT transitions (GT states); β decay can access states at excitation energies lower than the decay Q-value, and neutrino-induced reactions have very small cross-sections. However, one should note that β-decay has a direct access to the absolute GT transition strengths B(GT) from a study of half-lives, Q_β-values, and branching ratios.

In contrast, the complementary charge-exchange (CE) reactions, such as the (p,n) or $(^3\mathrm{He},t)$ reactions at intermediate beam energies and 0°, can selectively excite GT states up to high excitation energies in the final nucleus. In recent $(^3\mathrm{He},t)$ measurements, one order-of-magnitude improvement in the energy resolution has been achieved. This has made it possible to make one-to-one comparisons of GT transitions studied in CE reactions and β decays. Thus, GT strengths in $(^3\mathrm{He},t)$ reactions can be normalized by the β-decay values.

4.1 Study of Gamow-Teller Transitions in Charge-Exchange Reactions

Studies of GT strengths by the β^--type (p,n) reaction started in the 1980s using proton beams at intermediate energies. They provided rich information on the overall GT strength distributions up to the energy region of the GT giant resonances (GTR) having their center at $E_x \approx$ 8-15 MeV [13]. However, individual transitions were poorly studied due to the limited energy resolution ($\approx$ 300 keV) in (p,n) reactions. Therefore, it was not easy to calibrate the unit cross-section $\hat{\sigma}_{\rm GT}$ [see Eq. (4.1)] by using standard B(GT) values from β-decay studies on a level-by-level base [14].

The studies using $(^3\mathrm{He},t)$ reaction are performed at the high energy-resolution facility of RCNP, Osaka, consisting of high-dispersion beam line "WS course" [15] and the "Grand Raiden" spectrometer [16] using a beam from the $K = 400$ "Ring Cyclotron" [17]. The reaction performed at the intermediate incoming energy of 140 MeV/nucleon and at 0° is a unique tool for the study of

GT transitions owing to the high selectivity of exciting GT states and the high energy-resolution. Unlike the (p,n) reaction that has been used for the study of GT transitions, the emitted tritons can be momentum analyzed by using a magnetic spectrometer.

In addition, we apply dispersion matching techniques to improve the energy resolution as well as angular resolution in the spectrum obtained [18, 19, 20, 21]. By applying these matching techniques, a resolution better than the momentum (energy) spread of the beam can be realized. For a typical beam energy resolution of 120 keV, a resolution of ≈ 30 keV is achieved in the $(^3\mathrm{He},t)$ spectrum. The ion-optical concepts of the matching conditions are described in Ref. [4].

With this one order-of-magnitude better resolution achieved in the $(^3\mathrm{He},t)$ reaction, we can now study GT and Fermi states that were not resolved in the pioneering (p,n) reactions (see Fig. 4). As a result, detailed comparison with β-decay results is now possible.

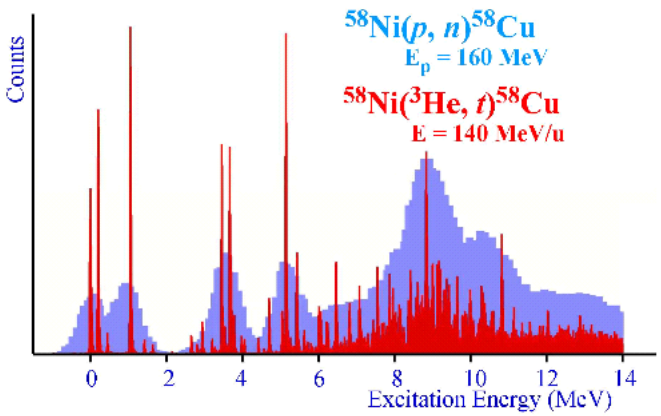

Figure 4: Energy spectra of charge-exchange reactions at 0°. The broad spectrum is from ^{58}Ni$(p,n)^{58}$Cu reaction measured in 1980's [13]. In the recent ^{58}Ni$(^3\mathrm{He},t)^{58}$Cu reaction [43] fine structure and sharp states have been observed up to the excitation energy of 13 MeV. The proton separation energy (S_p) is at 2.87 MeV. A increase of continuum is observed above $E_x = 6$ MeV.

4.2 Properties of High-resolution (^{3}He,t) Reaction

In CE reactions at intermediate incoming energies of more than 100 MeV/nucleon, the reaction mechanism becomes simple and the $\sigma\tau$ part of the effective interaction becomes dominant. As a result, at momentum transfer $q = 0$ there is a close proportionality between the cross-sections and the B(GT) values. This close proportionality that was first established in (p,n) reactions at intermediate energies of $120-200$ MeV [22, 14] was also observed in the $(^3\mathrm{He},t)$ reaction [4]

$$\frac{d\sigma_{\mathrm{GT}}}{d\Omega}(0) = \hat{\sigma}_{\mathrm{GT}}(0)B(\mathrm{GT}), \tag{4.1}$$

where $\hat{\sigma}_{\mathrm{GT}}(0)$ is a unit (differential) cross section for the GT transition at the momentum transfer $q = 0$ ($\approx 0°$).

The validity of the proportionality [Eq. (4.1)] was examined by comparing the GT transition strengths in the $(^3\mathrm{He},t)$ spectra to the B(GT) values from mirror β decays. Good proportionality

of $\approx 5\%$ was demonstrated for "$L = 0$" transitions with $B(\mathrm{GT}) \geq 0.04$ in studies of the $A = 26$, 27, and 34 nuclear systems [23, 24, 25, 26].

In a few specific transitions, however, larger deviations ($20 - 40\%$) from the proportionality were observed [26, 27]. The DWBA calculations performed using the transition matrix elements from shell-model calculations showed that the contribution of the Tensor interaction is responsible for these deviations from proportionality. It was found that in these cases two major $\Delta L = 0$ configurations, each of them having a large $\sigma\tau$ matrix element, contribute destructively to the GT transition strength. Then, the contribution of the $\Delta L = 2$ configurations activated by the $T\tau$ interaction is not negligible [26].

Although there are exceptions, the B(GT) values from the (^{3}He,t) CE reactions usually agreed with the β-decay B(GT) values by applying only one normalization parameter [4]. Owing to the high energy-resolution and the close proportionality given by Eq. (4.1), the (^{3}He,t) reaction is recognized as an excellent tool for the study of GT transitions in nuclei, especially of the strengths to discrete states up to high excitation region. In addition, one obtains information on the widths of the discrete states.

5. Gamow-Teller Response Functions for p-shell Nuclei

It is expected that the response of nuclei to GT transitions varies considerably reflecting the structures of initial and final nuclei. Here we show high energy-resolution (^{3}He,t) spectra obtained on a few p-shell nuclei at 0° and the intermediate energy of 140 MeV/nucleon, where the reaction mechanism is mainly one step. At 0° the dominant excitations are $\Delta L = 0$ transitions. Therefore, in the region of $E_x \leq 20$ MeV, where the main part of the "structured" GT strengths are expected, almost all $\Delta L = 0$ transitions, except for the excitation of the IAS caused by the τ-type Fermi operator, are GT excitations caused by the $\sigma\tau$ operator. In addition, due to the proportionality, the 0° spectra provide us with a good empirical representation of the GT strength functions. Due to the low level density, we can observe the GT states in p-shell nuclei as individual states. However, when these states are situated above the particle separation energies (either S_p or S_α), they can have a particle decay width. We will find that the transition strengths in these nuclei are strongly related to the cluster structure.

5.1 Gamow-Teller transitions in $A = 7$ nuclei

The main feature of the 0°, ^{7}Li(^{3}He,t)^{7}Be spectrum shown in Fig. 5(a) is the excitation of the two low-lying states. They are the $J^\pi = 3/2^-$ g.s and the $1/2^-$, 0.429 MeV first excited state [28]. These states are stable against particle-emission. Since the ground states of ^{7}Li and ^{7}Be are isobaric analog states, the transition strength between them is the incoherent sum of the Fermi and GT transitions.

The $\log ft$ values of β-decay transitions from the g.s of ^{7}Be to the g.s and the $1/2^-$, 0.478 MeV first excited state have been measured with good accuracy. They are the analogous transitions to those observed in the ^{7}Li(^{3}He,t) reaction. From these $\log ft$ values and assuming $B(\mathrm{F}) = 1$, we obtain $B(\mathrm{GT}) = 1.20$ and 1.07 for the g.s-g.s and g.s-first excited state transitions, respectively, using Eq. (3.3). These large B(GT) values and the concentration of the GT strength in these transitions suggest that the $J^\pi = 3/2^-$ g.s and the $1/2^-$, 0.429 MeV state are LS-partner states.

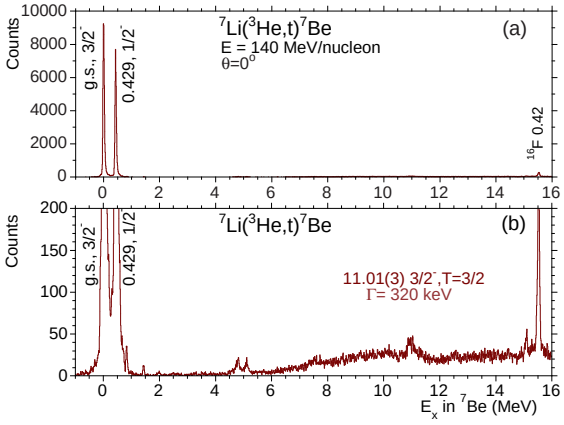

Figure 5: Energy spectra for the ^{7}Li(^{3}He,t)^{7}Be reaction at 0° on two vertical scales. a) The excitations of the $J^\pi = 3/2^-$ g.s and the $1/2^-$, 0.429 MeV excited state are the dominant features. b) The same 0° spectrum, but the vertical scale is expanded by a factor of fifty. The weakly excited $J^\pi = 3/2^-$, $T = 3/2$ state is observed at 11.01(3) MeV.

If we magnify the vertical scale by a factor of fifty, we can identify the weakly excited $J^\pi = 3/2^-$, $T = 3/2$ state at 11.01(3) MeV [see Fig. 5(b)]. This state is the IAS of the g.s of ^{7}He and ^{7}B [28]. The weak excitation of this state suggests that the g.s of the $T = 1/2$, ^{7}Li (and ^{7}Be) and the g.s of the $T = 3/2$, ^{7}He (and ^{7}B) have rather different spatial shapes. It has been reported that the strength of the analogous GT transition in the β^+ direction, i.e., from the g.s of ^{7}Li to the g.s of ^{7}He, observed in the (d,^{2}He) reaction is also very weak [29].

It should be noted that the energy difference between the $J^\pi = 3/2^-$ and $1/2^-$ *LS*-partner states is as small as 430 keV. Since the spin-orbit force is proportional to $-(1/r)dV/dr$, *LS*-partners with a large spatial extension tend to have a smaller splitting. Therefore, it is suggested that the ground states of ^{7}Li and ^{7}Be are rather diffuse.

5.2 The "odd mass Hoyle state" in $A = 11$ nuclei

The nuclei ^{11}B and ^{11}C are mirror nuclei. As shown in Fig. 6(a), the GT strength observed in the 0°, ^{11}B(^{3}He,t)^{11}C spectrum was fragmented. It was found that the fragmentation can be roughly understood by the coupling of a $p_{3/2}$ proton hole (for ^{11}B) or neutron hole (for ^{11}C) to the ^{12}C core. The coupling to the 0^+ g.s in ^{12}C produces the $J^\pi = 3/2^-$ ground states in ^{11}B and ^{11}C, and the coupling to the 2^+ first excited state at 4.44 MeV will produce a multiplet of states with $1/2^-$, $3/2^-$, $5/2^-$ and $7/2^-$. The $1/2^-$, $3/2^-$, $5/2^-$ states can be reached from the $3/2^-$ g.s by GT transitions. As reported in [30], the GT strength distribution was well reproduced by a classical shell-model calculation using the Cohen-Kurath interaction [31] with the introduction of a quenching factor, and also by an *ab initio* no-core shell-model calculation including a three-nucleon interaction [32, 33]. It should be noted that the latter could reproduce the absolute B(GT) strengths without introducing the quenching factor that was needed in the calculation given in Ref. [31].

Because of the excellent energy-resolution in the (^{3}He,t) experiment, a peak observed at 8.4 MeV in an earlier (p,n) experiment [31] was resolved into 8.105 and 8.420 MeV states in agreement with [34]. It was found that there was almost no strength in the transition to the second excited $J^\pi = 3/2^-$ state at 8.105 MeV, although the transition from the ^{11}B g.s with $J^\pi = 3/2^-$ is allowed by the J^π selection rule. We can see this state only by magnifying the vertical scale by a factor of thirty as shown in Fig. 6(b). Interest in this state is not only due to its weak excitation, but also its absence in the shell-model calculations. These features strongly suggest that this 8.105 MeV state has a completely different spatial structure from the other strongly excited states.

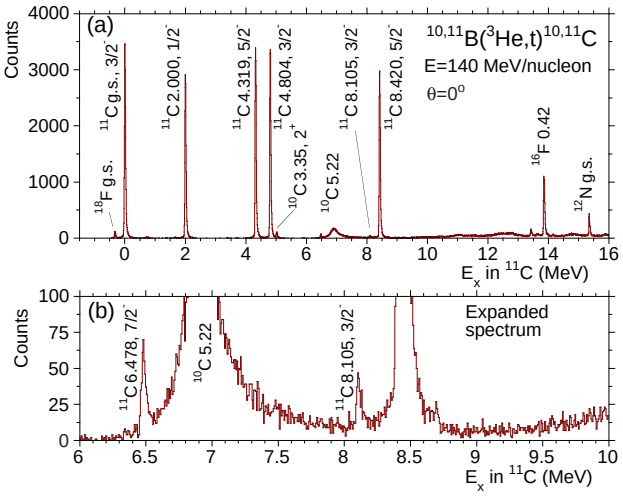

Figure 6: Energy spectra from the ^{11}B(^{3}He,t)^{11}C reaction at 0° on two scales. a) The spectrum up to $E_x = 16$ MeV. b) The expanded $6-10$ MeV region. The weakly excited $J^\pi = 3/2^-$, 8.105 MeV state is observed.

The answer came from recent calculations within the antisymmetrized molecular dynamics (AMD) framework. It was shown that the second excited $3/2^-$ state in ^{11}B and ^{11}C and the first excited 0^+ state at 7.65 MeV in ^{12}C have a strong similarity from the viewpoint of cluster structure [35]. As is well known, this 7.65 MeV, 0^+ state, the "Hoyle state," is situated just above the three α threshold and is interpreted as a dilute gas state of three weakly interacting α particles [36, 37, 38]. It plays an essential role in the formation of ^{12}C by the triple alpha reaction in the Cosmos. Correspondingly, the AMD calculation shows that the second excited $3/2^-$ states in ^{11}B and ^{11}C have the well-developed cluster structures of $2\alpha+^3$H and $2\alpha+^3$He with dilute density, respectively. Therefore, these states may be called "odd mass Hoyle states." The similarity of the structures of these states was suggested experimentally by the similarity of the angular distributions of these states in the ^{11}B and ^{12}C(d,d') reactions [39].

6. Combined study of β-decay and CE reaction

In the rp-process of nucleosynthesis, proton-rich pf-shell nuclei with $T_z = -1$ and smaller are involved. Although new results from various β-decay experiments are coming out, due to small production rate of these nuclei in the region of far-from-stability, the information from β-decay study itself is not always enough. By combining the results from β decay with the results from high-resolution (^{3}He,t) experiments, studies of GT transitions become fruitful. Here, we report the comparison of these two results for the $T_z = \pm 1 \rightarrow 0$ GT transitions in the pf-shell nuclei. We also show the complementary $T_z = \pm 2 \rightarrow \pm 1$ studies using the (^{3}He,t) reaction and β-decay. We have reported $T_z = +1 \rightarrow 0$ GT transitions in $A = 46, 50$, and 58 nuclear systems [40, 41, 42, 43] and the β-decay studies of mirror $T_z = -1 \rightarrow 0$ transitions have also been partly reported [44].

6.1 Isospin symmetry and analogous transitions

The Gamow-Teller (GT) transitions starting from stable as well as proton-rich unstable pf-shell nuclei play an important role in the core-collapse stage of type II supernovae [2]. However, our experimental study of the GT transitions starting from unstable nuclei with $T_z = -1$ or -2 is rather

poor; accurate β-decay half-lives have been measured for several $T_z = -1$ and -2 nuclei [45], but the determination of GT transition strengths, B(GT)s, have been out-of-reach in decay studies. This is due to the small production rate of such far-from-stability nuclei, and also the small f-factors in the feedings to higher excited states, which makes the accurate determination of branching ratios difficult.

Under the assumption that isospin T is a good quantum number, an analogous structure is expected for nuclei with the same mass A but with different T_z (isobars). The corresponding states in isobars are called isobaric analog states (or simply analog states), and are expected to have the same nuclear structure. Transitions connecting corresponding analog states are also analogous and have corresponding strengths (see e.g. Ref. [46]).

6.2 (^{3}He,t) reactions on $T_z = +1$ nuclei at RCNP and the mirror β-decay studies at GSI

The $T_z = +1 \rightarrow 0$ GT transitions were measured on target nuclei ^{42}Ca, ^{46}Ti, ^{50}Cr, and ^{54}Fe in the (^{3}He,t) reaction, while $T_z = -1 \rightarrow 0$ GT transitions were studied in the β decay of $T_z = -1$ mirror nuclei ^{42}Ti, ^{46}Cr, ^{50}Fe, and ^{54}Ni. The isospin symmetry is schematically shown in Fig. 7 for the $A = 54$ transitions.

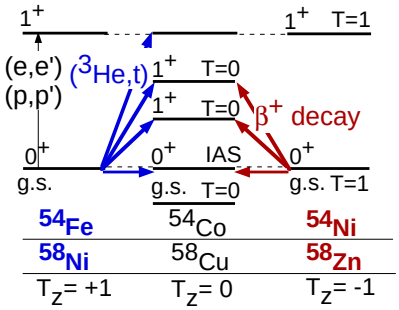

Figure 7: Schematic illustration of the isospin symmetry GT transitions in the "$T = 1$ system" for $A = 54$ and 58. The $T_z = \pm 1 \rightarrow 0$ transitions can be studied by the (^{3}He,t) reaction and β decay, respectively, for the pf-shell nuclei. Coulomb displacement energies are removed to show the isospin symmetry structure.

In order to compare results from these $T_z = \pm 1 \rightarrow 0$ GT transitions up to high excitation energies, it is important to achieve a good resolution in the (^{3}He,t) reaction to identify each transitions, while it is important to get high statistics in the β-decay measurements. This is illustrated in Fig. 8 for the $A = 54$ mirror GT transitions. The ^{54}Co spectrum observed in the ^{54}Fe(^{3}He,t) reaction [42] is shown in Fig. 8(a). As mentioned, the peak yields (or heights of peaks) are almost proportional to the B(GT) values. In the mirror β decay, i.e., in the decay of ^{54}Ni, it is expected that the branching ratios to the higher excited states are hindered by the phase-space factor (f-factor) shown in Fig. 8(b). The transition strength in the β decay is proportional to $1/t_i$, where t_j is the partial half-life for the GT transition to the jth excited state and is related to B_j(GT) by Eq. (3.4) Since λ^2 and K are constant, the "β-decay spectrum" showing the yields in the β decay can be deduced by multiplying the ^{54}Fe(^{3}He,t) spectrum with the f-factor. The estimated ^{54}Ni β-decay energy spectrum is shown in Fig. 8(c). Suppression of the feeding to higher excited states is obvious.

The $T_z = -1 \rightarrow 0$ β-decays of ^{42}Ti, ^{46}Cr, ^{50}Fe, and ^{54}Ni and their delayed γ rays were studied in order to measure the feeding ratios up to higher excitations and accurate half-lives [44]. It should be noted that in these measurements, we study the mirror GT and Fermi transitions that are observed in (^{3}He,t) reactions on $T_z = +1$ nuclei ^{42}Ca, ^{46}Ti, ^{50}Cr, and ^{54}Fe.

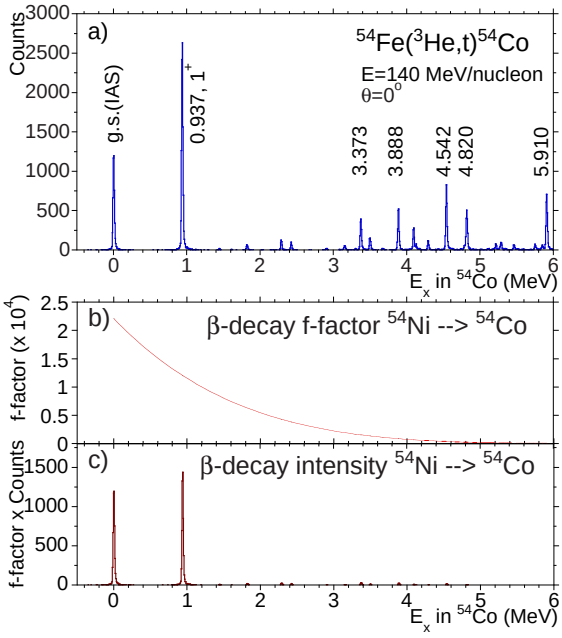

Figure 8: (a) The 0° spectrum of ^{54}Fe(^{3}He,t)^{54}Co reaction. Major $L = 0$ states are indicated by their excitation energies in MeV. (b) The f-factor for the ^{54}Ni β decay, calculated from the decay Q-value of 8799(50) keV. (c) The estimated strength distribution of ^{54}Ni β decay (^{54}Ni β-decay spectrum). Note that the IAS is stronger by a factor of ≈ 5 in the real β-decay measurement due to the different coupling constants in the β decay and the (^{3}He,t) reaction.

The experiment was performed as part of the RISING stopped beam campaign [47] at the FRagment Separator (FRS), GSI, Darmstadt. Beams of ^{42}Ti, ^{46}Cr, ^{50}Fe, and ^{54}Ni were produced by the fragmentation process from a primary 680 MeV/nucleon ^{58}Ni beam of 0.1 nA on a Be target. Each beam was well separated by the FRS facility and ions were implanted into an active stopper system consisting of three layers of double-sided silicon strip detectors (DSSDs). They were surrounded by the RISING γ-ray array composed of 15 EUROBALL cluster Ge detectors. The overall γ-ray detection efficiency was about 15% at 1.33 MeV.

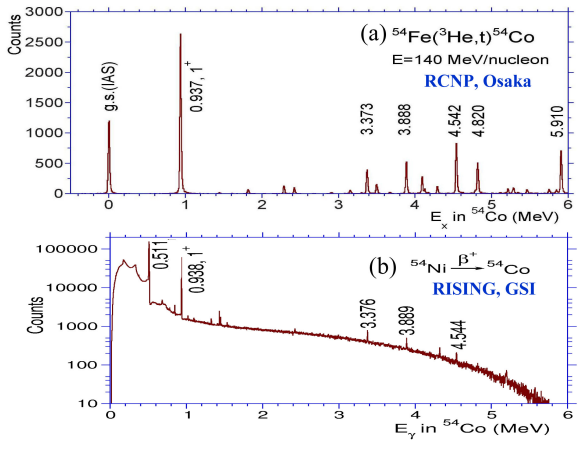

Figure 9: (a) The 0°, ^{54}Fe(^{3}He,t)^{54}Co spectrum. Major excited $L = 0$ states are indicated by energies in MeV. (b) γ-ray spectrum at RISING, GSI, measured in coincidence with the β particles from the ^{54}Ni decay. The existence of γ-ray peaks and CE-reaction peaks at corresponding energies suggests a good mirror symmetry of $T_z = -1 \rightarrow 0$ and $T_z = +1 \rightarrow 0$ GT transitions.

Due to the high production rate for ^{54}Ni and the good detection efficiency of the RISING setup high-energy delayed γ rays could be seen [Fig. 9(b)] at the energies corresponding to the GT states observed in the ^{54}Fe(^{3}He,t)^{54}Co measurement [42]. Even γ rays higher than 4 MeV could be identified. A good symmetry is suggested for the $T_z = \pm 1 \rightarrow 0$ GT transitions.

An interesting feature of the $M1$ γ decays from the excited $T = 0$, 1^+ states in the $T_z = 0$ daughter nucleus ^{54}Co is that they mostly decay directly to the $T = 1$, 0^+, g.s (the IAS of ^{54}Ni, g.s). This can be mainly explained by the fact that the coupling constant (the g-factor) of the $\sigma\tau$ component in the $M1$ operator is much larger than that of the σ component. In the $T_z = 0$ nucleus ^{54}Co, the $\sigma\tau$ component can contribute only to the $M1$ γ decays with $T = 0 \to 1$, but not to the $T = 0 \to 0$ decays, where the latter can be caused by the weak σ component.

6.3 The ^{52}Cr(^{3}He,t) reaction at RCNP and the mirror ^{52}Ni β decay at GANIL

The isospin symmetry of analog states and the analogous GT and Fermi transitions in the "$T = 2$ quintet" are shown in Fig. 10 for the $A = 52$ isobars.

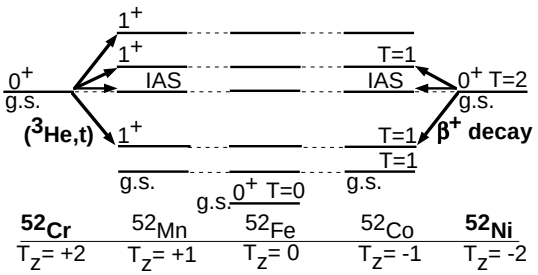

Figure 10: Schematic view of the analog states and the isospin symmetry transitions in the mass $A = 52$, $T = 2$ quintet, where the Coulomb energy is removed. The (^{3}He,t) reaction studies the $T_z = +2 \to +1$ GT transitions and the Fermi transition to the isobaric analog state (IAS), while the β decay can study the analogous transitions with $T_z = -2 \to -1$.

The $T_z = +2 \to +1$, ^{52}Cr(^{3}He,t)^{52}Mn experiment was performed at RCNP, Osaka. A resolution of $\Delta E = 29$ keV achieved by using matching techniques was crucial in separating the IAS and the nearby 1^+, GT states [see Fig. 11(a)]. Using the proportionality [Eq. 4.1] and the "merged analysis" [41] that uses the $T_{1/2}$ value (40.8 ± 0.2 ms in the β decay of ^{52}Ni [45]) as an input, accurate B(GT) values are derived.

Assuming good isospin symmetry of the $T_z = \pm 2 \to \pm 1$ GT transitions, the "β-decay spectrum" of the $T_z = -2$ nucleus ^{52}Ni can be deduced by multiplying the calculated f-factor to the (^{3}He,t) spectrum on the $T_z = +2$ nucleus ^{52}Cr shown in Fig. 11(a). Furthermore, by adding the width corresponding to the experimental resolution of the delayed-proton measurement, a spectrum shown in Fig. 11(b) was obtained. It should be noted that the proton decay from the IAS is suppressed by the isospin selection rule (see the figure caption of Fig. 11). By assuming an appropriate suppression factor, we could well reproduce the delayed-proton spectrum of the ^{52}Ni β decay shown in Fig. 11(c).

7. Gamow-Teller Strengths in pf-shell Nuclei

As mentioned, GT strength distributions as a function of excitation energy, i.e., the GT strength spectrum, can be largely different in different mass A systems reflecting individual nuclear structures of initial and final nuclei.

In nuclei heavier than nickel region (mass $A \geq 60$), we usually see concentration of GT strength at around $E_x \geq 10$ MeV, which is usually called GT resonances (GTRs) [13], while in nuclei lighter than *sd*-shell, we hardly see a prominent GTR structure. Therefore, it is expected that we can observe the development of the GTR structure for the nuclei in the f-shell region.

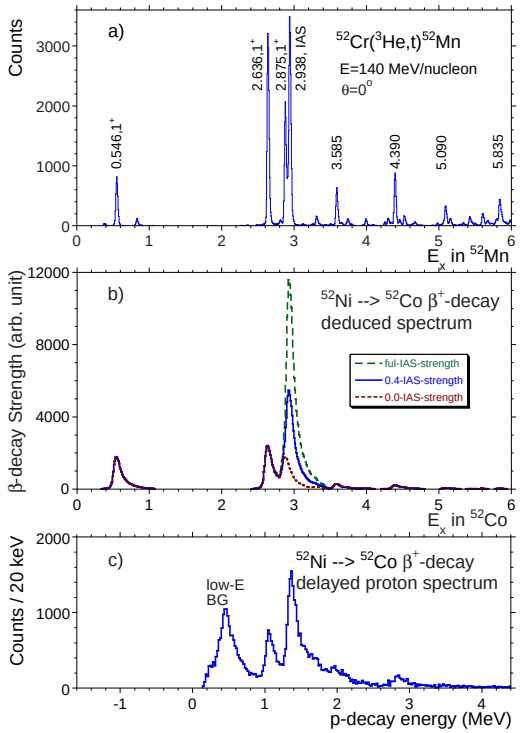

Figure 11: (a) The ^{52}Cr(^{3}He,t)^{52}Mn spectrum for events within scattering angles $\Theta \leq 0.5^{\circ}$. Major $L = 0$ states, most probably the GT states, are indicated by their excitation energies in MeV. (b) The estimated strength distribution of ^{52}Ni β decay that is obtained by multiplying the calculated f-factor to the ^{52}Cr(^{3}He,t) spectrum of the figure (a). The proton decay from the $T = 2$, IAS in the $T_z = -1$ nucleus ^{52}Co is not allowed by the isospin selection rule; the decay is possible only through the $T = 1$ isospin impurity. Therefore, the peak corresponding to the proton decay of the IAS should be suppressed. (c) The delayed-proton spectrum obtained in the ^{52}Ni, β-decay measurement (from Ref. [45]).

The main configurations of the GTRs of usual $N > Z$ nuclei are of *p*-*h* nature. The observation of a GTR at much higher E_x ($\approx 8-15$ MeV) than the energy gap of $j_<$ and $j_>$ orbits ($\approx 3-6$ MeV) can be partly explained by the repulsive nature of the *p*-*h* interaction [48]. In addition, IV-type interactions are repulsive. Therefore, the GR structure in the IV-type GT excitations can be pushed up further.

However, in light $f_{7/2}$-shell nuclei we notice that GT excitations with pure *p*-*p* configurations can be realized as a rare case due to the CE nature of the excitation and also due to the fact that only two configurations consisting of $f_{7/2}$ orbit with the $j_>$ nature and $f_{5/2}$ orbit with the $j_<$ nature can contribute to the GT transitions. Then, there comes out a naive question how the attractive *p*-*p* (or *h*-*h*) interaction competes with the repulsive *p*-*h* interaction in the IV-type GT excitation.

We find that such a competition can be ideally studied by examining the mass dependence of the GT strength distribution starting from the $N = Z+2$ ($T_z = 1$) even-even $f_{7/2}$-shell nuclei to the $N = Z$ ($T_z = 0$) odd-odd nuclei, where T_z, defined by $(N-Z)/2$, is the z component of isospin T. We can study for $A = 42, 46, 50$, and 54 systems, where initial nuclei are ^{42}Ca, ^{46}Ti, ^{50}Cr, and ^{54}Fe, respectively. As A increases, the $f_{7/2}$ orbit will be filled gradually on top of the $Z = N = 20$, ^{40}Ca inert core while the $f_{5/2}$ orbit is always kept open (see Fig. 12).

Since the initial and final T_z values are identical for all cases, it is expected that the total GT strengths are not so different [6]. In addition, the strength distribution is not affected by the isospin Clebsch-Gordan coefficients that re-distribute the GT strength among the final $T = T_0 - 1$, T_0, and $T_0 + 1$ states [4, 49] with T_0 being the isospin of the initial state.

In these nuclei, the GT excitations all have the same nature of $\nu f_{7/2} \rightarrow \pi f_{7/2}$ and $\nu f_{7/2} \rightarrow \pi f_{5/2}$. However, in the $A = 42$ system, we notice that the two final configurations, i.e., both

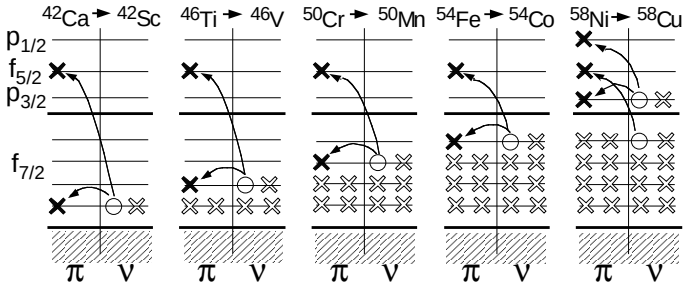

Figure 12: Allowed configurations of GT$_-$ transitions starting from $T_Z = +1$ to $T_Z = 0$ nuclei in the pf-shell, where most simplified shell structure is assumed. The filling of protons (π) and neutrons (ν) are shown by open crosses. The newly created holes and particles after the transitions are shown by the open circles and filled crosses, respectively.

$(\pi f_{7/2}, \nu f_{7/2})$ and $(\pi f_{5/2}, \nu f_{7/2})$, have attractive *p*-*p* nature. As A increases, the latter looses its *p*-*p* nature and tends to have the repulsive *p*-*h* nature, as is clear in the $A = 54$ system (see Fig. 12). The former also looses its *p*-*p* nature, but in $A = 54$ it again has the attractive *h*-*h* nature. In the $A = 58$ system, the *p*-*p* type $(\pi p_{3/2}, \nu p_{3/2})$ and $(\pi p_{1/2}, \nu p_{3/2})$ configurations further take part in, and additional conflict with the repulsive $(\pi f_{5/2}, \nu f_{7/2})$, *p*-*h* configuration is expected.

With the splendid resolutions of $25 - 40$ keV, the GT strength distributions of the transitions starting from the $T_z = +1$ target nuclei with $A = 42 - 58$ were studied in detail as shown in Fig. 13 [50]. The analysis of the angular distribution for each transition suggested that most of the well excited states have the $L = 0$ nature and they are the GT excitations. We see that the Gamow-Teller (GT) strength that is concentrated in one low-lying state in the lightest odd-odd $N = Z$ f-shell nucleus ^{42}Sc moves up to higher energy region with the increase of mass A and finally forms a GR structure in the heaviest f-shell nucleus ^{54}Co and also in ^{58}Cu.

From Fig. 13, it is clear that the GT strengths in ^{42}Sc are pulled down and accumulated to the 0.61 MeV, 1^+ state. This feature can be explained by the fact that both $(\pi f_{7/2}, \nu f_{7/2})$ and $(\pi f_{5/2}, \nu f_{7/2})$ configurations have the attractive *p*-*p* nature in ^{42}Sc (see Fig. 12). On the other hand in ^{54}Co, in which the $(\pi f_{5/2}, \nu f_{7/2})$ configuration has clearly the repulsive *p*-*h* nature, the main part of the GT strength is pushed up. The $(\pi f_{7/2}, \nu f_{7/2})$ configuration has the attractive *h*-*h* nature, but only 10 to 15 % of the observed GT strength remains in the first 1^+ state. The overall repulsive nature of the residual interaction in ^{54}Co can be understood by the numbers of available transitions that make the $(\pi f_{5/2}, \nu f_{7/2})$, *p*-*h* configuration and the $(\pi f_{7/2}, \nu f_{7/2})$, *h*-*h* configuration; assuming a simple shell structure, they are 48 and 16, respectively. In ^{58}Cu, due to the additional $(\pi p_{3/2}, \nu p_{3/2})$ and $(\pi p_{1/2}, \nu p_{3/2})$ configurations, strengths are also observed at $E_x = 3 - 5$ MeV. However, the dominance of the repulsive *p*-*h* type $(\pi f_{5/2}, \nu f_{7/2})$ configuration still pushes the main part of the GT strength to the higher E_x region.

It is now clear that the repulsive nature of the *p*-*h* type configurations mainly contribute to the formation of the GR structures in nuclei. In CE reactions, however, *p*-*p* type configurations can also be realized as a rare case. In such cases the GT strengths are concentrated to the transition to the lowest-lying GT state, as we have seen in the ^{42}Ca(^{3}He,t)^{42}Sc measurement. The $\log ft$ value of the mirror GT transition that has been studied in the ^{42}Ti β-decay to the 0.61 MeV, 1^+ state is as

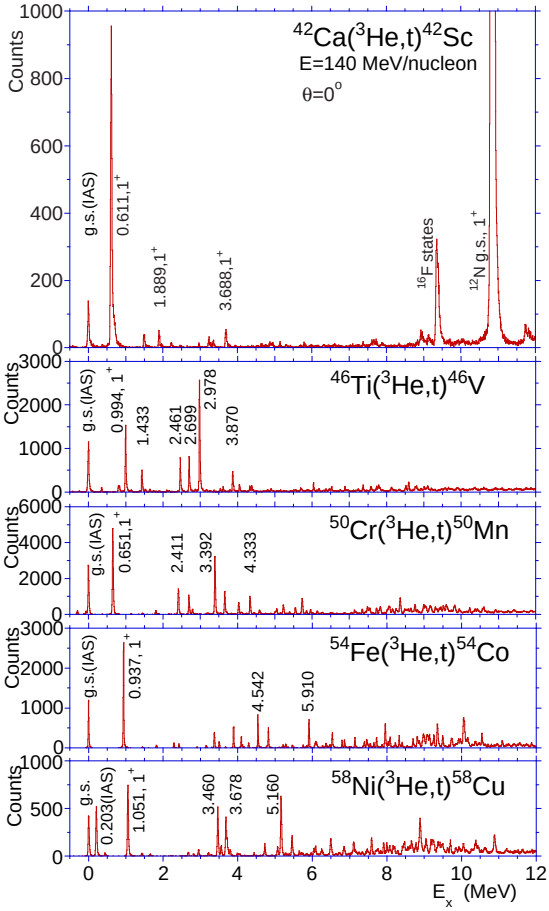

Figure 13: High energy-resolution (^{3}He,t) spectra for $T_z = +1$ target nuclei in the pf shell. An energy resolution of ≈ 30 keV is obtained. The result of the angular distribution suggests that most of the prominent states are $L = 0$ GT states. The vertical scale is normalized by the heights of the IAS peaks all having $B(\mathrm{F}) = 2$. Thus, peak heights are almost proportional to B(GT). As the mass number A increases, the GT states are more fragmented and more GT strength is found in a higher energy region of $7-12$ MeV.

small as 3.18(11), a value similar with the super-allowed Fermi transition. Therefore, we suggest that this strong GT transition is called by the name "super-allowed GT transition", and the 0.61 MeV, 1^+ state "super-allowed GT state."

Other examples of the super-allowed GT transitions are the g.s$-$g.s GT transition of the ^{18}Ne β^+) decay to ^{18}F, and the g.s$-$g.s GT transition of the ^{6}He β^- decay to ^{6}Li. They have the logft values of 3.1 and 2.9, respectively. It should be noted that all of these final states have the p-p type configurations on top of the doubly LS-closed shell structure, i.e., the structure of the super-allowed GT state.

8. Gamow-Teller Resonance Structures in ^{118}Sb

As shown in Fig. 4, the broad bump-like structure of GT-GRs observed in ^{58}Ni$(p,n)^{58}$Cu reaction measured in 1980's [13] was resolved into fine structure and sharp states in the recent ^{58}Ni(^{3}He,t)^{58}Cu measurement [43]. It is then our interest whether such fine structures can be found even in heavier nuclei if they are studied with the high energy resolution of the (^{3}He,t) reaction. The level density of GT states is another interest. We select ^{118}Sn as the target nucleus. It is a representative spherical medium-heavy nucleus.

The ^{118}Sn(^{3}He,t)^{118}Sb spectrum taken at 0° with a resolution of 30 keV is shown in Fig. 14. The g.s of ^{118}Sb has the $J^\pi = 1^+$, and the g.s$-$g.s transition starting from the 0^+ g.s of ^{118}Sn is the

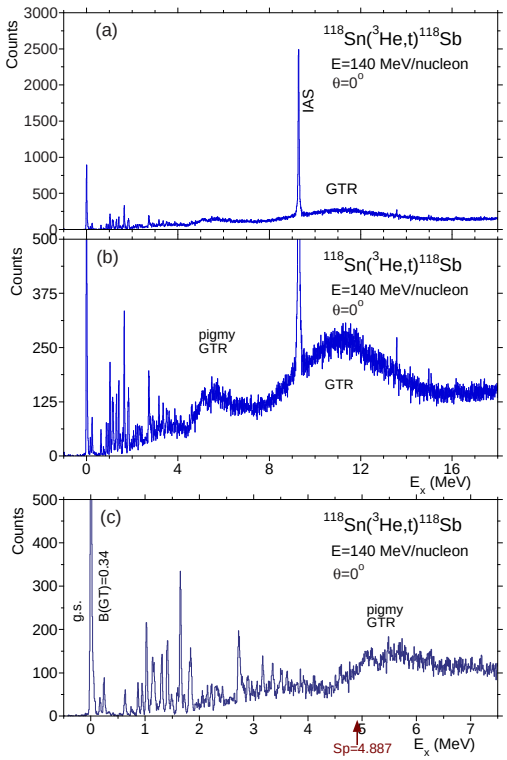

Figure 14: (a) ^{118}Sn(^{3}He,t)^{118}Sb spectrum. Discrete g.s, low-lying states, and the IAS are prominent. (b) ^{118}Sn(^{3}He,t)^{118}Sb spectrum with an expanded vertical scale. (c) ^{118}Sn(^{3}He,t)^{118}Sb spectrum with an expanded vertical as well as energy scale.

GT transition. Since the B(GT) value of this transition is well determined in the β-decay study of ^{118}Sb, we can get the unit GT cross section $\hat{\sigma}^{\mathrm{GT}}(0^\circ)$. Then, using the Eq. 4.1, the B(GT) values can be deduced for the transitions to excited states. In this spectrum, the $E_x = 51$ keV, 3^+ state in ^{118}Sb was clearly recognized as a skirt of the g.s peak, and we expect to get a reliable cross section for the g.s$-$g.s transition.

The proton separation energies S_p is 4.887(3) MeV in ^{118}Sb. Therefore, there should be no decay width for the excited states below this energy and we should see discrete states. We see that the low-lying states below $E_x = 2$ MeV are mostly well separated. In the energy region between $2-4$ MeV, however, we see fine structures, but the spectra are not decomposed into states even with our resolution of 30 keV. Taking our energy resolution of 30 keV, we suggest that the level density of the GT states in this region is higher than one per 30 keV at $E_x = 4$ MeV. Above this energy region, only the IAS has been clearly observed as discrete state. The IAS is apparently wider than the g.s, showing the spreading and decay width due to the isospin impurity in the IAS.

In ^{118}Sb, it is interesting to see that the GT strength is divided into four parts, i.e., the g.s, the clustering states in $E_x = 1-2$ MeV, $2-4$ MeV, a bump-like structure in $4-8$ MeV and the GT-GR structure in $E_x = 8-15$ MeV. The bump-like structure in $4-8$ MeV is called the pigmy GT resonance [51]. It is stressed that the existence of such an interesting structure even in a nucleus with a relatively high mass of $A = 118$ is a challenge to the understanding of nuclear structure.

9. Summary

The processes caused by the weak interaction happen at a "δ-function-like point" in space. Therefore, the "reaction mechanism" involved in the process is very simple and we even don't

use the word "reaction mechanism", for example, for the β decay. As a result, the GT transition strengths are proportional to reduced transition strengths B(GT). Then, the key issue is how to obtain the B(GT) values of GT transitions.

In many cases of astrophysical processes, GT transitions to highly excited states play significant contributions, but the study of them by means of β decay is not possible due to the limited Q-value of the decay. One of the answers was to use CE reactions at intermediate incoming energies and 0° to study these GT transitions. In the pioneering (p,n) reactions performed under these conditions, GT resonances showing a bump-like structure were observed at around $E_x = 10$ MeV. In addition, it was found that there is a close proportionality between the obtained cross-sections at the momentum transfer $q = 0$ ($\approx 0°$) and the B(GT) values.

With the improvement in the energy resolution in the β^--type CE reaction (^{3}He,t) performed at 140 MeV/nucleon at RCNP, we have started to see the detailed information on GT transitions; fine structures of GT excitations, even those of GT resonances, and also the width of each state. In addition, by comparing the cross-sections at 0° with the B(GT) values of the analogous GT transitions obtained in mirror β decays for *sd*-shell nuclei, a close proportionality was also observed in the (^{3}He,t) reaction. Owing to the proportionality, the B(GT) values can be deduced up to high excitation energies once a standard B(GT) value is provided by the β decay.

The GT transitions in pf-shell nuclei, not only those starting from stable nuclei, but also unstable nuclei are of interest in nuclear-astrophysics. However, in the pf-shell region, the β-decay B(GT) values have larger uncertainties; only $T_{1/2}$ values were relatively reliable. By the introduction of isospin symmetry in the study of GT transitions, the (^{3}He,t) measurements and the β-decay studies are now tightly connected. Newly obtained β-decay results at the fragment-separator facilities (GSI and GANIL) are complementary and could be analyzed together.

Acknowledgments

The high-resolution (^{3}He,t) experiments were performed at RCNP, Osaka. The author is grateful to the participants in the experiments and the accelerator group of RCNP. This work was supported in part by MEXT, Japan under Grants No. 18540270 and No. 22540310 and also by the Japan-Spain collaboration program of JSPS and CSIC. Discussions with B. Rubio (Valencia), W. Gelletly (Surrey), P. von Brentano (Köln), B. Blank (Bordeaux) and K. Muto (TIT) are acknowledged.

References

[1] F. Osterfeld, Rev. Mod. Phys. **64**, 491 (1992), and references therein.

[2] K. Langanke and G. Martínez-Pinedo, Rev. Mod. Phys. **75**, 819 (2003).

[3] A. Heger *et al.*, Phys. Rev. Lett. **86**, 1678 (2001).

[4] Y. Fujita, B. Rubio and W. Gelletly, Prog. Par. Nucl. Phys. **66**, 549-606 (2011), and references therein.

[5] A.M. Bernstein, Advances in Nuclear Physics **3** (1969) 325.

[6] M.N. Harakeh, A. Van Der Woude, *Giant Resonances* Oxford Studies in Nucl. Phys. 24 (Oxford University Press, Oxford, 2001).

[7] J.C. Hardy and I.S. Towner, Phys. Rev. C **79**, 055502 (2009).

[8] J.C. Hardy and I.S. Towner, Nucl. Phys. News **16**, 11 (2006).

[9] I.S. Towner and J.C. Hardy, Phys. Rev. C **66**, 035501 (2002).

[10] L. Zamick and D. C. Zheng, Phys. Rev. C **37**, 1675 (1988).

[11] A. R. Edmonds, *Angular Momentum in Quantum Mechanics* (Princeton University Press, Princeton, 1960).

[12] B. Rubio and W. Gelletly, Lec. Notes in Phys. **764**, 99-151 (2009).

[13] J. Rapaport and E. Sugarbaker, Annu. Rev. Nucl. Part. Sci. **44**, 109 (1994).

[14] T.N. Taddeucci *et al.*, Nucl. Phys. **A469**, 125 (1987).

[15] T. Wakasa et al., Nucl. Instrum. Methods Phys. Res. A **482**, 79 (2002).

[16] M. Fujiwara et al., Nucl. Instrum. Methods Phys. Res. A **422**, 484 (1999).

[17] See web site http://www.rcnp.osaka-u.ac.jp.

[18] Y. Fujita *et al.*, Nucl. Instrum. Meth. Phys. Res. B **126**, 274 (1997); and references therein.

[19] Y. Fujita *et al.*, Nucl. Phys. **A687**, 311c (2001).

[20] H. Fujita *et al.*, Nucl. Instrum. Meth. Phys. Res. A **469**, 55 (2001).

[21] H. Fujita *et al.*, Nucl. Instrum. Meth. Phys. Res. A **484**, 17 (2002).

[22] W.G. Love and M.A. Franey, Phys. Rev. C **24**, 1073 (1981).

[23] Y. Fujita *et al.*, Phys. Rev. C **67**, 064312 (2003).

[24] R. Zegers *et al.*, Phys. Rev. C **74**, 024309 (2006).

[25] Y. Fujita *et al.*, Phys. Rev. C **59**, 90 (1999).

[26] Y. Fujita *et al.*, Phys. Rev. C **75**, 057305 (2007).

[27] A.L. Cole *et al.*, Phys. Rev. C **74**, 034333 (2006).

[28] D.R. Tilley, C.M. Cheves, J.L. Godwin, G.M. Hale, H.M. Hofmann, J.H. Kelley, C.G. Sheu, and H.R. Weller, Nucl. Phys. **A708**, 3 (2002).

[29] N. Ryezayeva *et al.*, Phys. Lett. B **639**, 623 (2006).

[30] Y. Fujita *et al.*, Phys. Rev. C **70**, 011306(R) (2004).

[31] T.N. Taddeucci *et al.*, Phys. Rev. C **42**, 935 (1990).

[32] P. Navrátil and W.E. Ormand, Phys. Rev. C **68**, 034305 (2003).

[33] P. Navrátil *et al.*, Phys. Rev. Lett. **99**, 042501 (2007).

[34] F. Ajzenberg-Selove and J.H. Kelley, Nucl. Phys. **A506**, 1 (1990).

[35] Y. Kanada-En'yo, Phys. Rev. C **75**, 024302 (2007).

[36] A. Tohsaki, H. Horiuchi, P. Schuck, and G. Röpke, Phys. Rev. Lett. **87**, 192501 (2001).

[37] Y. Funaki, A. Tohsaki, H. Horiuchi, P. Schuck, and G. Röpke, Phys. Rev. C **67**, 051306(R) (2003).

[38] M. Chernykh, H. Feldmeier, T. Neff, P. von Neumann-Cosel, and A. Richter, Phys. Rev. Lett. **98**, 032501 (2007).

[39] T. Kawabata *et al.*, Phys. Rev. C **70**, 034318 (2004).

[40] T. Adachi *et al.*, Phys. Rev. C **73**, 024311 (2006).

[41] Y. Fujita *et al.*, Phys. Rev. Lett. **95**, 212501 (2005).

[42] T. Adachi *et al.*, Phys. Rev. C **85**, in press (2012).

[43] H. Fujita *et al.*, Phys. Rev. C **75**, 034310 (2007).

[44] F. Molina, B. Rubio, Y. Fujita, and W. Gelletly, AIP Conf. Proc. **1265**, 49 (2010).

[45] C. Dossat, B. Blank *et al.*, Nucl. Phys. A **792**, 18 (2007).

[46] A. Bohr and B. Mottelson, *Nuclear Structure* (Benjamin, New York, 1975), Vol. 2, Chap. 6, and references therein.

[47] "Stopped Beam" RISING experimental campaign at GSI, spokespersons: P.H. Regan, J. Gerl, and H.J. Wollersheim.

[48] J.P. Schiffer and W.W. True, Rev. Mod. Phys. **48**, 191 (1996).

[49] Y. Fujita *et al.*, Phys. Rev. C **62**, 044314 (2000).

[50] T. Adachi *et al.*, Nucl. Phys. **A788**, 70c (2007).

[51] K. Pham *et al.*, Phys. Rev. C **51**, 526 (1995).